2D PERIODIC PHOTONIC NANOSTRUCTURES INTEGRATED IN 40 µm THIN CRYSTALLINE SILICON SOLAR CELLS

Christos Trompoukis[1, 2], Ounsi El Daif[4], Valerie Depauw[1], Twan Bearda[1], Kris Van Nieuwenhuysen[1], Jonathan Govaerts[1], Hariharsudan Sivaramakrishnan Radhakrishnan[1], Roberto Martini[1,2], Stefano Granata[1,2], Ivan Gordon[1] , Robert Mertens[1] , Jef Poortmans[1, 2, 3]

1. IMEC, Kapeldreef 75, B-3001 Belgium
2. KUL, Departement Elektrotechniek – ESAT, Kasteelpark Arenberg 10, B-3001 Leuven, Belgium
3UHasselt, Martelarenlaan 42, 3500 Hasselt, Belgium
4. Qatar Environment and Energy Research Institute (QEERI) 5825 Doha, Qatar

ABSTRACT: Two-dimensional (2D) periodic photonic nanostructures are fabricated by nanoimprint lithography (NIL) and dry plasma (*Dry-NIL*) etching on 40 µm thick epitaxially-grown crystalline silicon (c-Si) foils, resulting in nanostructures with a parabolic profile. These nanostructures are integrated in a 40 µm thick double side contacted c-Si/aSi:H heterojunction solar cell architecture. The front side is processed when the foil is attached to the parent substrate while the back side is processed when the foil is bonded to the glass carrier. Although the efficiency of the nanopatterned cell was lower compared to the random pyramid textured cells it had a better absorption and spectral response for long wavelengths, highlighting a better light trapping behavior.
Keywords: Light trapping, c-Si, a-Si, Heterojunction, optical properties.

1 INTRODUCTION

In order to increase the competitiveness of photovoltaics (PV) with respect to the cost of grid electricity supplied by fossil fuels, nuclear power or even other renewable sources, a combination of reduced fabrication costs and high solar cell efficiencies is required [1]. With crystalline silicon (c-Si) being an important part of the module cost, using thinner c-Si substrates has been a major trend. However, this trend poses two main challenges: issues with handling and processing of such thin substrates within the current c-Si solar cell fabrication methods and the material's poor light absorption due to the indirect band-gap of c-Si.

Regarding the fabrication of thin c-Si layers, the epitaxial growth of 40 µm foils with high lifetimes has been reported [2, 3]. Such thin-film c-Si layers are held by a carrier substrate, thus eliminating the handling issues while enabling the processing on module level. Moreover, the fabrication of 43 µm thin solar cells with efficiencies up to 19% has already been reported [4]. Those cells incorporate a conventional light trapping scheme based on the formation of random pyramids on the front side of the device. However, micron sized random pyramids on one hand reach their limitations [5, 6] due to insufficient light trapping and on the other hand the material waste (a few microns) during their fabrication becomes critical with such thin layers. Therefore, other approaches for highly efficient advanced light trapping are needed.

Various theoretical works suggest that light trapping beyond the commonly accepted limit of Lambertian light scattering is possible through the use of periodic photonic nanostructures [7, 8]. The fabrication of such nanostructures, their optical performance and their passivation has been studied [9-12]. However, integrating them in a solar cell device is shown to be challenging due to a critical trade-off between optical and electrical properties. In fact, by modifying the photoactive material's surface and by introducing extra process steps, surface nanopatterns are shown to affect the functioning of crystalline-silicon (c-Si) solar cells. On the one hand, nanopatterns are expected to increase the cells' photon absorption, and thus to affect positively their short-circuit current density (Jsc), and on the other hand they are shown to negatively impact the cells' open-circuit voltage Voc and fill-factor FF [13].

In this contribution we report on the integration of 2D photonic nanostructures and the effect of this light trapping scheme on the optical and electrical properties (absorption, current, voltage, FF) of the cells. A benchmarking of the nanopatterned cells with respect to random pyramid textured cells is done.

2 EXPERIMENTAL DETAILS

Two dimensional photonic nanostructures were fabricated by soft thermal nanoimprint lithography (NIL) [14] and etching. Regarding NIL, a thermoplastic polymer resist was spin coated on the substrates and a thermal imprint of a periodic array of circular openings was performed at 130˚C as presented in [9-12]. Regarding the etching of silicon, dry plasma (*Dry-NIL*) was used in order to transfer the pattern from the etch-mask to silicon. A capacitively coupled single wafer reactive ion etching (RIE) system was used. The period of the nanostructures was around 850 nm. For the formation of the random pyramid texturing, 20% TMAH in water at 80 ˚ C was used.

The 40 µm epifoils were fabricated as presented in [3] and the cell fabrication (flow shown in Figure 1) included the processing of the front side on the parent substrate, the bonding to a glass carrier, the detachment of the foil and the process of the rear side of the cell. In particular, the front side texturing (periodic nanostructures or random pyramids) was done as described earlier. Intrinsic and n-type doped amorphous silicon (i/n+ a-Si) was deposited by PECVD for

the passivation and front surface field formation. Indium tin oxide (ITO) was sputtered in order to form the antireflection coating, also serving as the transparent conductive oxide. Ti/Pd/Ag contact were e-beam evaporated through shadow masks as the front metallisation. After the front side processing, the foil was detached and bonded to a glass carrier, giving access to the back side processing sequence. During bonding, holes that had been pre-drilled in the glass were aligned to the front side busbars to be able to contact the front side of the cells at the end. Intrinsic and p-type doped amorphous silicon (i/p+ a-Si) was deposited by PECVD for the passivation and the emitter formation. Regarding the back metal dielectric stack, ITO was sputtered and Ag was e-beam evaporated. Finally, the cells were separated by dicing the full cell stack and the glass carrier.

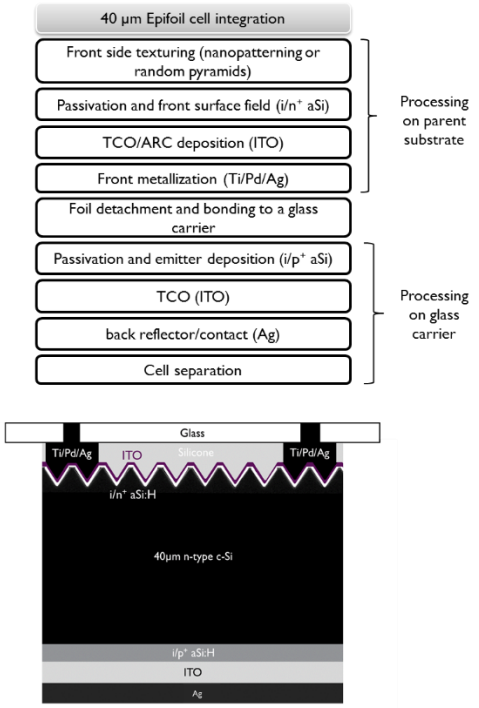

Figure 1. Epifoil double side contacted solar cell fabrication process flow sequence (up) and schematic cross section of the final stack (down).

The total epifoil area was 7x7 cm^2 bonded on a glass carrier sample with an area of 15.6 x 15.6 cm2. The nanopatterned area was 5 x 5 cm^2. After dicing, the cells had an area of 1.1 cm^2 including the busbar.

The topography was characterized with scanning electron microscopy (SEM). The optical properties of the nanopatterns were characterised by spectrally resolved reflectance measurements, within a wavelength range from 300 to 1170 nm using an integrating sphere. Absorption is then extracted as $A(\lambda) = 100 - R(\lambda) - T(\lambda)$. Since there was a full metal on the back, transmission was zero. The integrated values of absorption are the proportion of the solar photons absorbed over the range from 300 to 1200 nm taking into account the AM1.5 global tilt intensity distribution. The electrical performances of the cells were evaluated by quantum efficiency (EQE) measurements, and current–voltage (I–V) measurements under a calibrated AM1.5 solar simulator.

3 RESULTS AND DISCUSSION

Figure 2 shows the front textured topographies of the photonic nanostructures (*Dry-NIL*) with a parabolic profile and the micron scale random pyramids. In the SEM pictures, the films (aSi and ITO) deposited on top of the front side texturing are also visible.

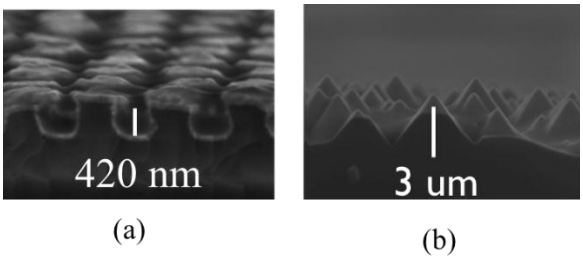

Figure 2. Topography of (a) *Dry-NIL* and (b) the reference random pyramid texturing.

The cell results are summarized in Table I. It should be noted that since the cells have an area of 1.1 cm^2, the parasitic effects which originate from the non-passivated diced edges become important. The efficiency of the random pyramid textured cell was higher than the nanopatterned cells. The random pyramid textured cell had a Voc of 675 mV while *Dry-NIL* showed a lower value of 635 mV. Following a similar trend, the fill factor (FF) reduced from 75 for the random pyramids to 73 for the nanopatterns. Regarding the current, the EQE was used for a more accurate extraction of the current: since the spot size used during the spectral response measurements was 0.54 mm wide, the measurement was localized towards the center of the cells, minimizing the effect from the unpassivated edges. By integrating the measured spectral response of the cells, the current which is mentioned in the parenthesis of Table 1 was calculated. In this way, a current of 32.6 mA/cm^2 was calculated for the random pyramids. The current was less (30.8 mA/cm^2) for the *Dry-NIL* due to a worse antireflective performance with respect to the random pyramids.

Table I. Solar cell characteristics. The Jsc values in the parenthesis correspond to the one extracted from EQE)

Sample	Jsc [mA/cm^2]	Voc [mV]	FF [%]	Eta [%]
Dry-NIL	25.2 (30.8)	635	73	11.8
Random pyramids	26.1 (32.6)	675	75	13.2

More precisely, the area fill fraction of the *Dry-NIL* shown in Figure 2 is low (part of the topography is flat) and therefore, as discussed in [11], the antireflective properties of this topography is expected to be low. In fact, the absorption (integrated value of 90 %) of the *Dry-NIL*, shown in Figure 3, was lower than the random pyramids (91.5 %).

The reason for such low current values is due to the parasitic absorption in the front side thin films. Both the 75 nm of ITO and the 30 nm of aSi are responsible for large part of the incoupled light being parasitically absorbed in this part of the cell. This is obvious from the very low EQE (Figure 3) of both cells for the short wavelengths of light.

Finally, from the absorption and EQE of the cells shown in Figure 3, we can see that the optical performance of the random pyramid texturing is better for the short wavelengths which results to a higher spectral response for this wavelength range (300-600 nm). However, for long wavelengths (900-1200 nm) the absorption and spectral response of the nanopatterned cell is better than the random pyramid cell, highlighting a better light trapping behavior.

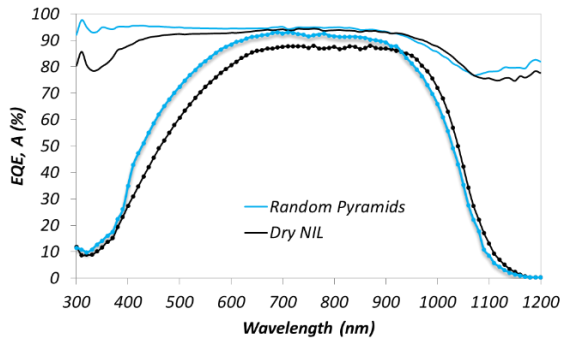

Figure 3. Absorption (solid lines) and EQE (lines with marker) for the random pyramid textured and *Dry-NIL* 40 µm cells.

4 CONCLUSION AND OUTLOOK

The integration of 2D periodic photonic nanostructures in a 40 µm thick epitaxial crystalline silicon solar cell was presented. The efficiency of the nanopatterned cell was lower compared to the random pyramid textured cells. However, we were able to show that thanks to the nanopattern, a better absorption and spectral response for long wavelengths was achieved, highlighting a better light trapping behavior with respect to the random pyramid texturing. With more process optimisation, better performance could be reached. Future process optimization include the reduction of the parasitic absorption losses on the front side, a better antireflective performance for the nanopatterned cells while maintaining the good light trapping performance and higher Voc by better passivated surfaces.

ACKNOWLEDGEMENTS

The authors acknowledge the financial support from Imec's industrial affiliation program. This work has been also partially funded from the European Union's Seventh Framework Programme for research, technological development and demonstration PhotoNVoltaics (Nanophotonics for ultra-thin crystalline silicon photovoltaics) under grant agreement No 309127.

REFERENCES:

[1] ITRPV, "International Technology Roadmap for Photovoltaic (ITRPV.net) Results 2011," Mar-2012. [Online]. Available: http://itrpv.net/.cm4all/iproc.php/Reports%20downloads/roadmap_itrpv_march_2012_full_web.pdf?cdp=a. [Accessed: 15-Jan-2013]

[2] F. Dross, K. Baert, T. Bearda, J. Deckers, V. Depauw, O. El Daif, I. Gordon, A. Gougam, J. Govaerts, S. Granata, R. Labie, X. Loozen, R. Martini, A. Masolin, B. O'Sullivan, Y. Qiu, J. Vaes, D. Van Gestel, J. Van Hoeymissen, A. Vanleenhove, K. Van Nieuwenhuysen, S. Venkatachalam, M. Meuris, J. Poortmans, Progr. Photovolt. Res. Appl 20 (2012) 770.

[3] Radhakrishnan HS, Martini R, Depauw V, Van Niuwenhuysen K, Debucquoy M, Govaerts J, Gordon I, Mertens R, Poortmans J. Improving the quality of epitaxial foils produced using a porous silicon-based layer transfer process for high-efficiency thin-film crystalline silicon solar cells. IEEE Journal of Photovoltaics 2013. DOI: 10.1109/JPHOTOV.2013.2282740

[4] J. H. Petermann, D. Zielke, J. Schmidt, F. Haase, E. G. Rojas, R. Brendel, Progr. Photovolt. Res. Appl 20, 1 (2012).

[5] Nelson, J., The Physics of Solar Cells (Imperial College Press, London 2003).

[6] P. J. Verlinden, M. Aleman, N. Posthuma, J. Fernandez, B. Pawlak, J. Robbelein, M. Debucquoy, K. Van Wichelen, J. Poortmans, Sol. Energ. Mat. Sol. 106 (2012) 37.

[7] A. Mellor, I. Tobias, A. Marti, M. J. Mendes, A. Luque, Progr. Photovolt. Res. Appl 19, (2011) 676.

[8] K. X. Wang, Z. Yu, V. Liu, Y. Cui and S. Fan, Nano Lett. 12 (2012) 1616.

[9] C. Trompoukis, A. Herman, O. El Daif, V. Depauw, D. Van Gestel, K. Van Nieuwenhuysen, I. Gordon, O. Deparis, J. Poortmans, in: Proceedings of SPIE photonics Europe, Brussels, Belgium, 16-19 April 2012, Photonics for Solar Energy Systems IV, pp. 84380R-84380R-10.

[10] C. Trompoukis, O. El Daif, V. Depauw, I. Gordon, J. Poortmans, Appl. Phys. Lett. 101 (2012) 103901.

[11] C. Trompoukis, O. El Daif, P. Pratim Sharma, H. Sivaramakrishnan Radhakrishnan, M. Debucquoy, V. Depauw, K. Van Nieuwenhuysen, I. Gordon, R. Mertens, J. Poortmans, Progr. Photovolt. Res. Appl. (2014) DOI: 10.1002/pip.2489.

[12] C. Trompoukis, I. Abdo, R. Cariou, I. Cosme, W. Chen, O. Deparis, A. Dmitriev, E. Drouard, M. Foldyna, E. Garcia-Caurel, I. Gordon, B. Heidari, A. Herman, L. Lalouat, K-D. Lee, J Liu, K. Lodewijks, F. Mandorlo, I. Massiot, A. Mayer, V. Mijkovic, J. Muller, R. Orobtchouk, G. Poulain, P. Prod'Homme, P. Roca i Cabarrocas, C. Seassal, J. Poortmans, R. Mertens, O. El Daif, V. Depauw, Phys. Status Solidi (a) (2014) DOI: 10.1002/pssa.201431180

[13] V. Depauw, X. Meng, O. El Daif, G. Gomard, L. Lalouat, E. Drouard, C. Trompoukis, A. Fave, C. Seassal, I. Gordon, IEEE J. Photovolt. 4 (2013) 215.

[14] S. Y. Chou, P. R. Krauss, P. J. Renstrom, Science 272 (1996) 85.